Sensitivity analysis of input ground motion on surface motion parameters in high seismic regions: A case of Bhutan Himalaya

Karma Tempa[1], Komal Raj Aryal[2], Nimesh Chettri[1], Giovanni Forte[3], Dipendra Gautam[4, *]

[1]Civil Engineering Department, College of Science and Technology, Royal University of Bhutan, Phuentsholing, Bhutan

[2]Faculty of Resilience, Rabdan Academy, Abu Dhabi, United Arab Emirates

[3]Department of Civil, Environmental and Architectural Engineering (DICEA), University of Naples Federico II, Naples, Italy

[4]Department of Civil Engineering, Institute of Engineering, Thapathali Campus, Kathmandu, Nepal

[*] *Correspondance*: Dipendra Gautam (dipendra01@tcioe.edu.np)

Abstract. Historical earthquakes have demonstrated that strong motion characteristics and local soil condition when coupled significantly influence seismic site response. Most of the Himalayan earthquakes have depicted anomalous behavior per the site conditions historically. Being one of the most active seismic regions on earth, the eastern fringe of the Himalaya has observed many devastating earthquakes and uneven damages were extensively reported. To this end, we present quantification of surface motion parameters for a soft soil deposit located at Phuentsholing city in western Bhutan. Using one dimensional site response analysis, sensitivity of ground motion variation is estimated for Bhutan. This study accounts for the earthquakes of moment magnitude between 6.6 and 7.5 with a wide variation of peak ground acceleration (PGA) even beyond 0.28g, which is the maximum PGA range suggested by the Global Seismic Hazard Map (GSHAP). To dissect the characteristics of six inputted ground motions on eight local ground conditions, sensitivity analysis is performed statistically. The statistical correlation of the response data sets and the linear regression model of the bedrock outcrop and the surface motion spectral acceleration along the stratified depth were examined to quantify the variation in surface motion parameters. The Results highlighted that the strong motions having PGA greater than 0.34 g demonstrate greater sensitivity leading to some anomalies in response parameters, resulting in attenuation of seismic site effect (amplification). The same scenario was observed for the PGA range below 0.1g.

Keywords: seismic site effect, amplification factor, soil fundamental period, sensitivity analysis, Bhutan.

1. Introduction

Bhutan is located in the eastern fringe of Hind-Kush-Himalaya. Historical earthquakes that occurred in the Hind-Kush-Himalayan region have resulted in enormous losses and damages (Gautam et al., 2016) and thus the impending earthquakes are certain to strike the region with detrimental consequences. The eastern fringe of Himalaya, i.e., Bhutan, and neighboring areas were strongly affected by significant earthquakes in the past, however, most of those occurred until the 18th century are not well-documented. The most recent events occurred on April 05, 2021 (M_w 5.0) in Samtse (South Bhutan) and in September 2009 Mongar earthquake (Mw 6.7) in eastern Bhutan. These earthquakes caused major damages in the eastern parts of Bhutan and considerably

affected the other parts of the Country (Chettri et al., 2021b). All the past earthquakes highlighted anomalous damage pattern to structures and infrastructures in various parts of the country, especially in the plain areas. Such evidence prompt indication of likely local site effects in Bhutan. So far, few studies on local seismic response have been conducted in Bhutan using a single strong motion but the studies mainly focused on the role of bedrock depth on ground response parameters (see e.g., Tempa et al., 2020; Tempa, Chettri, Gurung, et al., 2021). The ground motion response analysis may not adequately address the accuracy in predicting the response parameters due to limited information regarding site characteristics and their variations within the same soil column (Stevens et al., 2020). In the case of data scarce region such as Bhutan, the variation in terms of material characteristics can be possibly accounted for using sensitivity analysis. For this reason, this study quantifies the characteristics and effects of several strong ground motions to site effects depiction. Seismic ground response analysis fall in the Grade III approach of microzonation studies (e.g. ISSMGE 1999; Licata et al., 2018), it is widely used method widely by researchers for various applications in order to capture local ground effects or site conditions that can affect the estimate and prediction of ground motion characteristics (Chavez-Garcia et al., 1990; Lopez-Caballero et al., 2012, Gautam and Chamlagain 2016, Sil and Haloi 2018). The outcomes of such studies aim to provide local seismic hazard parameters which can be adopted for design of structures and infrastructures (Douglas, 2006). Ground response parameters typically characterize the complex nature of strong motion accelerograms using a simple expansion of predictive relationships. The two prominent deterministic and probabilistic approaches are widely used for seismic hazard studies globally. Previously, Tempa, Chettri, Gurung, et al. (2021) recommended the use of the deterministic approach that can estimate parameters under various earthquake occurrence scenarios. Notably, selecting a single ground motion considering amplitude only for seismic hazard analysis may not be a reliable approach to estimate site amplification. The selection of wide amplitude range and the assessment of likely fluctuation scenario for Bhutan is not done yet. Hence, ground motion parameters that are related to the amplitude are investigated to examine and predict the variability, often regarded as sensitivity, concerning mean values and associated scatter.

In this paper, sensitivity analysis of site response for specific soil conditions in Phuentsholing, Bhutan is explored by a statistical correlation function of the ground motion parameters for different earthquake shaking intensities. The study area is one of the major urban and commercial hubs in Bhutan Himalaya and seismic site effects on existing structures may have detrimental consequences due to inherent vulnerabilities of structures and infrastructures as well as due to the likely phenomenon such as amplification effects in loose soil deposits. To quantify the seismic site effects in terms of amplification of amplitude parameters, a range of time histories is selected, and site response parameters are estimated.

2. Seismicity and geology of the study area

The Himalayan region is one of the most seismically active regions on earth, which observes both large and moderate-sized events frequently (Drukpa et al., 2006). Bhutan is located in the eastern Himalayas formed due to the subduction of the Indian plate beneath the Eurasian Plate and spans from the low-lying Brahmaputra Plain to the high Tibetan Plateau. Most of the land area of Bhutan is underlain by the Main Himalayan Thrust (MHT), which runs along the entire length of the Himalayan arc. Historical earthquake catalog (see Fig. 1a) indicates that Bhutan has experienced several earthquakes of moment magnitude greater than 5.0 since early 1900, among them, the 1915 Trashigang (M_w 6.6), 1954 Trashiyangtse (M_w 6.4) in the 2009, Mongar (M_w 6.1) earthquake that occurred at 11 km east of Bhutan are the most notable ones. The 2011 Sikkim-Nepal earthquake (M_w 6.9)

also caused noticeable damage to building stocks in Bhutan (Chettri et al., 2021a). The earthquakes in the vicinity of the study area (Phuentsholing) include the 1981 Dagana (M_w 5.1) earthquake and the 2003 Haa earthquake (M_w 5.5). The most recent event occurred in Samtse in 2021 (M_w 5.1) affected Phuentsholing and the neighboring areas with an intensity level of IV in Modified Mercalli Intensity (MMI) scale. Continuity of seismic activities in Bhutan is attributed to the presence of major shear zones such as the Main Himalaya Thrust (MHT), Main Boundary Thrust (MBT), Main Central Thrust (MCT), and the South Tibetan Detachment System (STDS) (Long & McQuarrie, 2010) as shown in Figure 1a. The study area is within the Phuentsholing formation of Buxa group of the Lesser Himalaya mainly characterized by highly weathered dark grey to black slate and phyllite, thin interbeds of limestone with substantial amount of cream-colored dolomite and fine-medium quartzite, additionally consisting fine to medium grained conglomeratic quartzite interbedded with phyllite and dolomite towards the Rinchending area of Zone II. Hence, the lithological characteristic of the area indicates weak and highly unstable geology in the region. The presence of thrust faults in the proximity of the study area along the entire belt of the Lesser Himalayan units and the quaternary sediments in the south depict the area to be seismically active with the majority of the historical earthquake events concentrated within these geological units. In particular, this study focuses on Phuentsholing Thromde (city) of Chhukha dzongkhag (district) in Bhutan (Fig. 1c). The city is one of the major commercial hubs for trade with India. The proposed study area is observing rapid infrastructure development activities and urban expansion for residential, commercial, and industrial purposes. The Phuentsholing city covers an area of 15.6 km^2 and is located at 26.86°E and 89.39°N. The city has the population of 27,658 people, mostly distributed towards the peripheral international border area with a total of 2,263 residential and commercial buildings per the 2020 statistics (http://www.pcc.bt/index.php/). The seismic site characterization includes eight locations in the regions of Dhamdhara, Toorsa, and Rinchending in Phuentsholing, Bhutan. In this study, the sites are grouped into two main zones based on the geographical location and immediate availability of survey locations. These two zones also refer to the Local Area Plan (LAP) of Phuentsholing. The zones are Zone I: Dhamdhara I, Dhamdhara II, Toorsa I and Toorsa II, and Zone II: College of Science and Technology (CST) Football Ground, CST Hostel, Phajoding, and Monastery area. Among the 8 LAPs, Dhamdhara and Toorsa (Zone I) are in the same region in the western part of the city and Rinchending (Zone II) in the east.

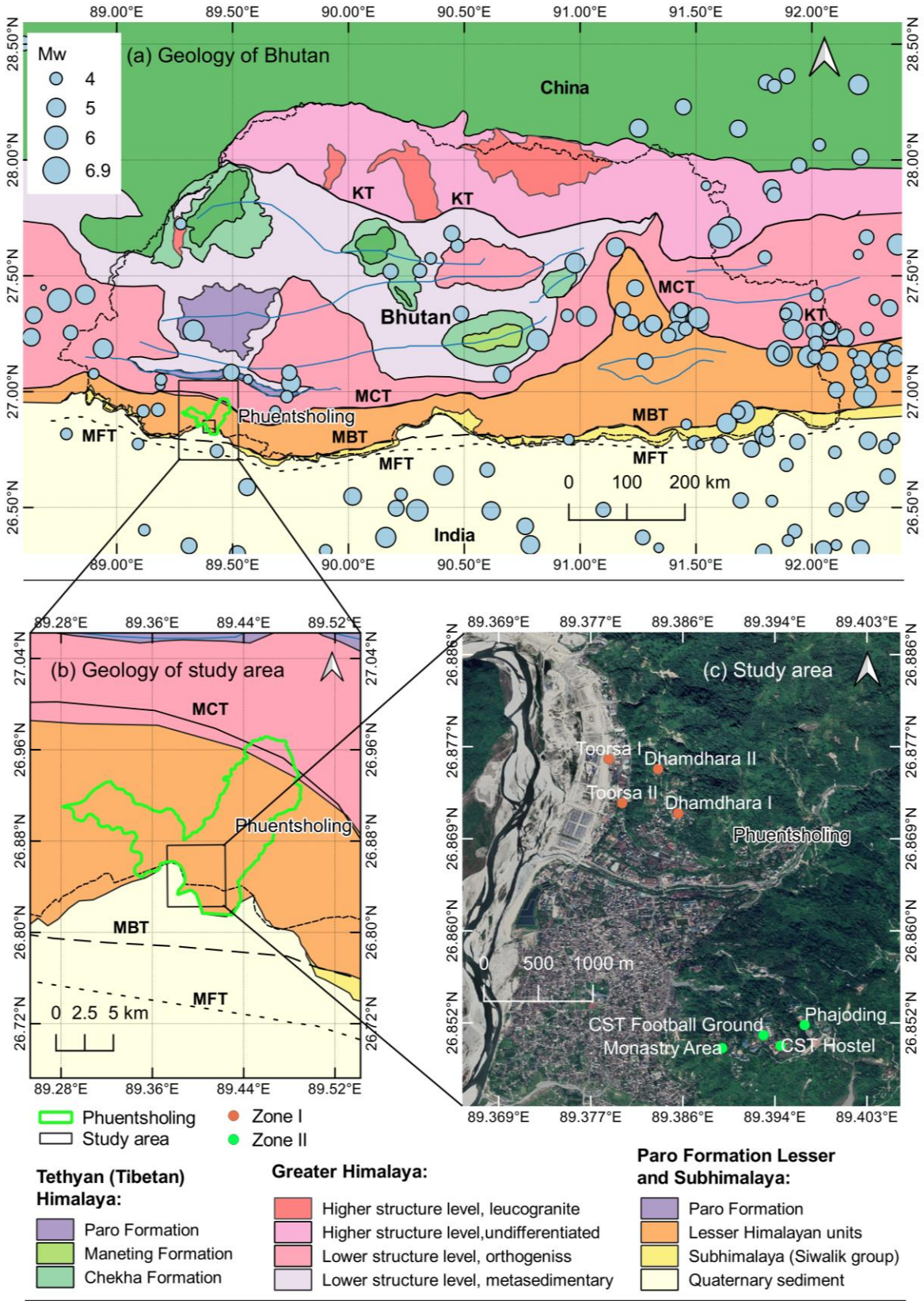

Figure 1: Geology and seismicity and the study area: (a) Geological map of Bhutan reproduced from McQuarrie et al. (2013) and seismicity, (b) Location of Phuentsholing and geology of the area, (c) Study area showing surveyed site using MASW (modified from Google Earth Pro 2021).

3. Materials and method

3.1 Geotechnical site characterization

The geotechnical reports collected by Phuentsholing municipality have 29 stratigraphic logs. From these records, the depth of the water table (GWT) was demarcated. Drilling log data showed the highest depth of the water table in the Dhamdhara area at 12.5 m to 16 m, whereas groundwater table in Rinchending area is at 5 m, followed by the Toorsa area at 0.5 m and 3 m, which is located near the riverbed. The depth of the water table is one of the essential input parameters used for 1D ground response analysis. Three drill holes are presented to typically illustrate the underground stratigraphy (Figure 2). Table 1 presents a summary of soil properties from laboratory testing of in-situ samples collected from the drill holes. The number of samples in each zone represents the total number of samples collected from all drill logs at various stratigraphic depths. All laboratory tests have been verified according to the Indian Standard Codes. Testing included physical identification, Atterberg limits, grain size distribution and direct shear testing. Field tests such as standard penetration resistance (SPT) and core cutter test were performed to determine resistance to penetration (SPT-N) and field density, respectively

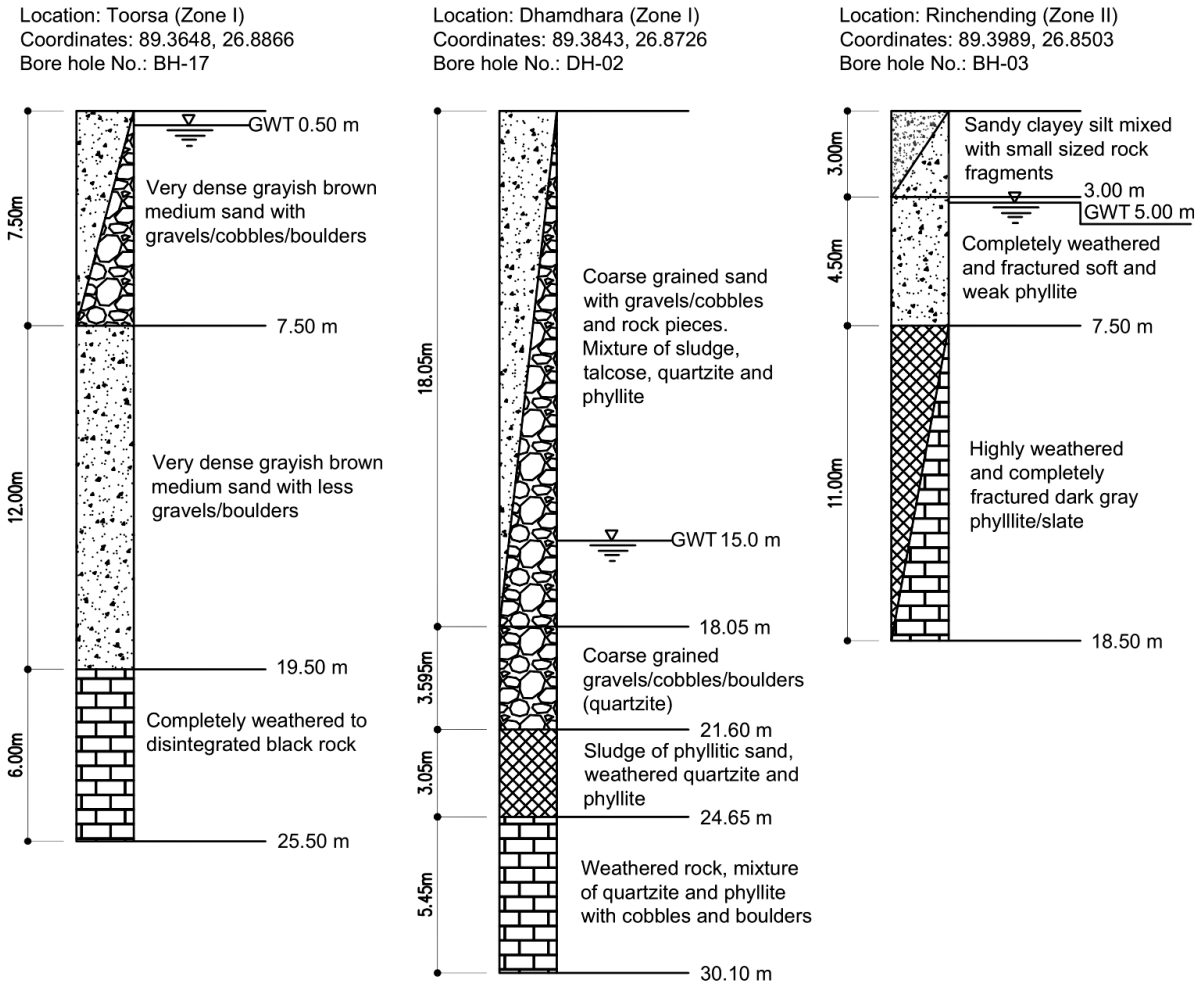

Figure 2: Typical borehole stratigraphy in Toorsa and Dhamdhara (Zone I) and Rinchingding (Zone II).

As shown in the stratigraphic logs, the upper strata comprise predominantly mixed coarse-grained soils characterized by dominant sand with considerable fraction of sand. The soil classification of the Phuentsholing area carried out by sieve analysis highlighted that most soils consist of 22.74% gravel, 74.89% sand, and 2.37% of the silt and clay. The sieve analysis results for the respective zones are shown in Fig. 3. The soils in Toorsa are non-plastic, as coarse-grained soils dominate the particle distribution, while the soils in Rinchending and Dhamdhara have low plasticity with a plasticity index (PI) of 6.5 and 10, respectively. The bulk density is 1.8 g/cm^3 in Toorsa, 1.64 g/cm^3 in Dhamdhara, and 1.33 g/cm^3 in Rinchending. The shear strength parameter, cohesion (c), ranges between 0-0.18 kg/cm^2, while the angle of internal friction (ϕ) in the study area is up to 35˚.

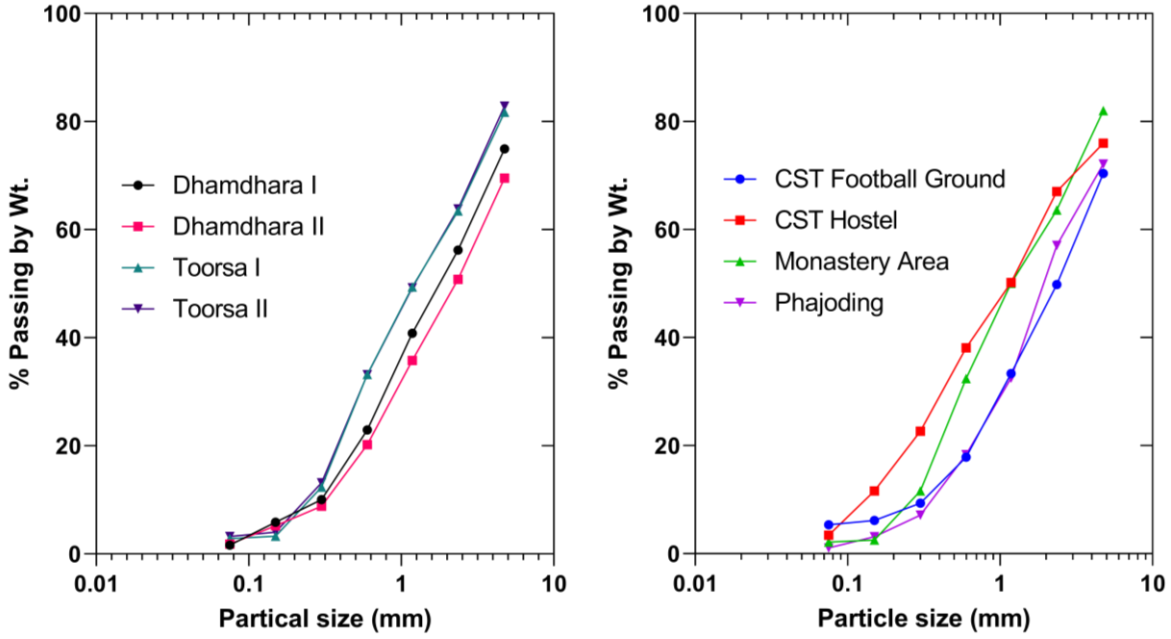

Figure 3: Representative grain size distribution curve for the study area.

Table 1. Average soil parameters in the study area.

Location	Testing methods	Soil parameters	No. of samples	Reference
Toorsa (Zone I)	Atterberg's limit	Non-plastic	86	IS: 2720 (Part 5)-1995
	Core cutter	Bulk density, γ_t = 1.8 g/cc Dry density, γ_d = 1.64 g/cc		IS:2720 (Part 29)-1975
	Direct shear	c = 0 ϕ = 35˚		IS: 2720 (Part 13)-1997
	SPT	*N* -value = 25 to 50		IS: 2131–1981
Dhamdhara (Zone I)	Atterberg's limit	Low plasticity (PI = 6.5)	28	IS: 2720 (Part 5)-1995
	Core cutter	Bulk density, γ_t = 1.64 g/cc Dry density, γ_d = 1.51 g/cc		IS:2720 (Part 29)-1975
	Direct shear	c = 0.073 kg/cm^2		IS: 2720 (Part 13)-1997

		$\phi = 31.44^{\circ}$		
	SPT	*N*-value = 19 to 37		IS: 2131–1981
Rinchending (Zone II)	Atterberg's limit	Low plasticity (PI = 10)	26	IS: 2720 (Part 5)-1995
	Core cutter	Bulk density, γ_t = 1.83 g/cc Dry density, γ_d = 1.70 g/cc		IS:2720 (Part 29)-1975
	Direct shear	c = 0.18 kg/cm^2 $\phi = 20\text{-}30^{\circ}$		IS: 2720 (Part 13)-1997
	SPT	*N*-value = 21 to <100		IS: 2131–1981

Shear wave velocity profiles from eight locations in the study area based on the multispectral surface wave analysis (MASW) and empirical correlation developed by Tempa, Chettri, Gurung, et al. (2021) are used to perform ground response analysis. According to the shear wave velocity profile, engineered bedrock (V_s > 800 m/s) lies at a depth of 150 m to 400 m as shown in Fig. 4. According to the parametric analysis carried out by Tempa et al. (2020), the site condition in the study area is classified into as ground type B per the Euro Code EC-08 and National Earthquake Hazards Reduction Program (NEHRP) with the majority of shear velocity ($V_{s,30}$) between 380–470 m/s, except for Phajoding, which has shear wave velocity of 584.76 m/s (Table 2).

Table 2. Site classification as per Euro Code EC-08

Zones	Sites	$V_{s,30}$ (m/s)	Ground Type
I	Dhamdhara I	386.43	B
	Dhamdhara II	435.92	B
	Toorsa I	439.54	B
	Toorsa II	464.30	B
II	CST football ground	426.76	B
	CST hostel	426.61	B
	Monastery area	446.20	B
	Phajoding	584.76	B
All	Bedrock	>800	A

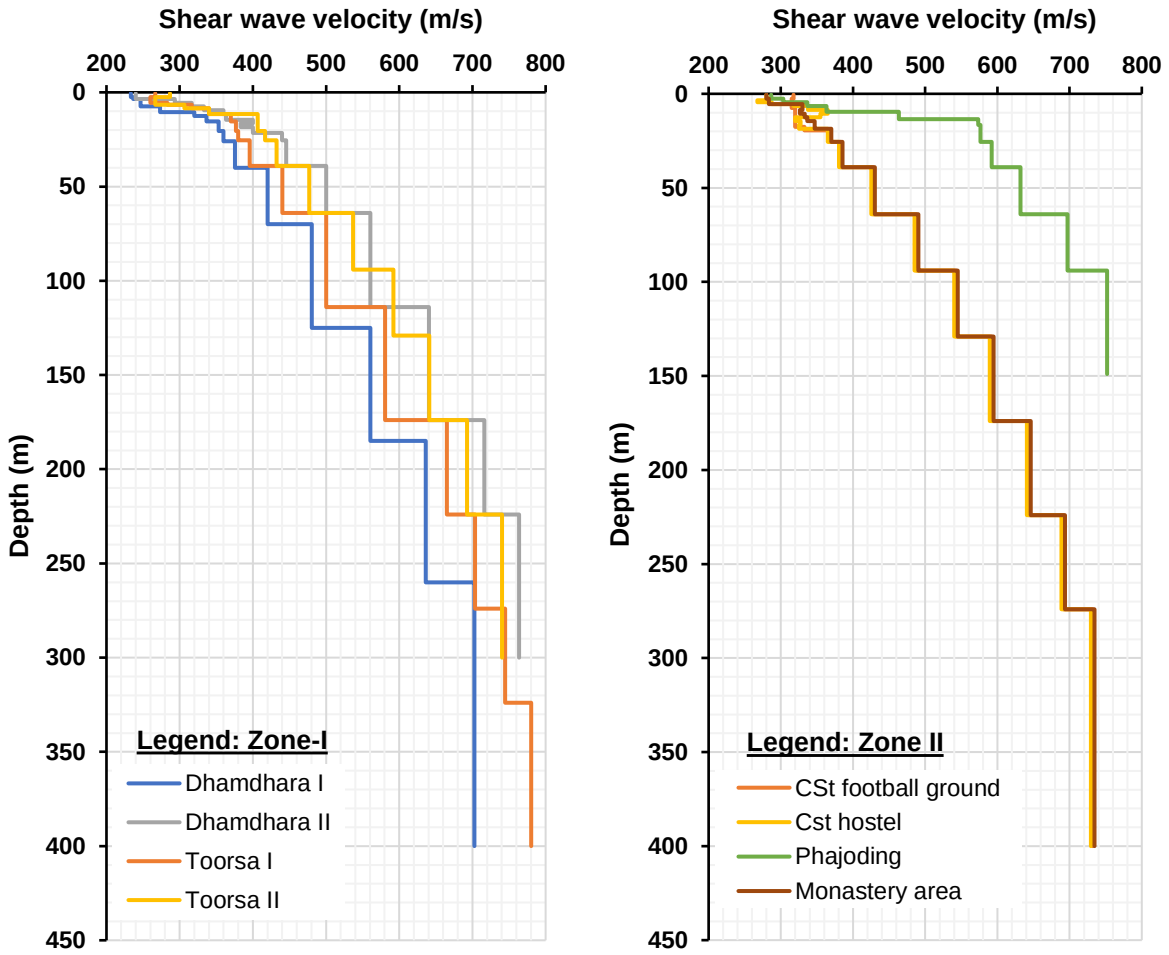

143

144 **Figure 4:** Shear wave velocity profile of study locations in Phuentsholing, Bhutan.

145 Dynamic properties of soils are influenced by shear modulus and damping and are defined by the
146 respective degradation models, regarded as the backbone curves. Figure 5 represents the dynamic soil model for
147 sand used in this study. Degradation models are well established by many investigators for different types of
148 soils affecting the response at low strain levels, (see e.g. Seed and Idriss, 1970; Vucetic and Dobry, 1991;
149 Darendeli, 2001; Dobry and Vucetic, 1982; Seed et al., 1986). A damped linear elastic model of the soil system
150 is used for the analysis. Due to soil nonlinearity for which the shear modulus is strain-dependent, ProShake
151 performs an iterative process on the linear model until both the moduli and damping ratios are compatible with
152 the average strains and convergence is achieved at the last iteration (Shafiee et al., 2011; Puri et al., 2018). The
153 nonlinear and hysteretic stress-strain behavior of soils under cyclic loading is approximated as a function of G_{sec}
154 and G_{max}. This predetermined estimation of G_{sec} or G and G_{max} is attributed by unit weight or bulk density, ρ,
155 and shear wave velocity, V_s ($G_{max} = \rho V_s^2$). Similarly, damping ratios are predicted as a function of G_{sec} or G
156 values. This estimation is achieved using an iterative procedure in the Proshake 2.0 program (EduPro Civil
157 Systems Inc., 2017).

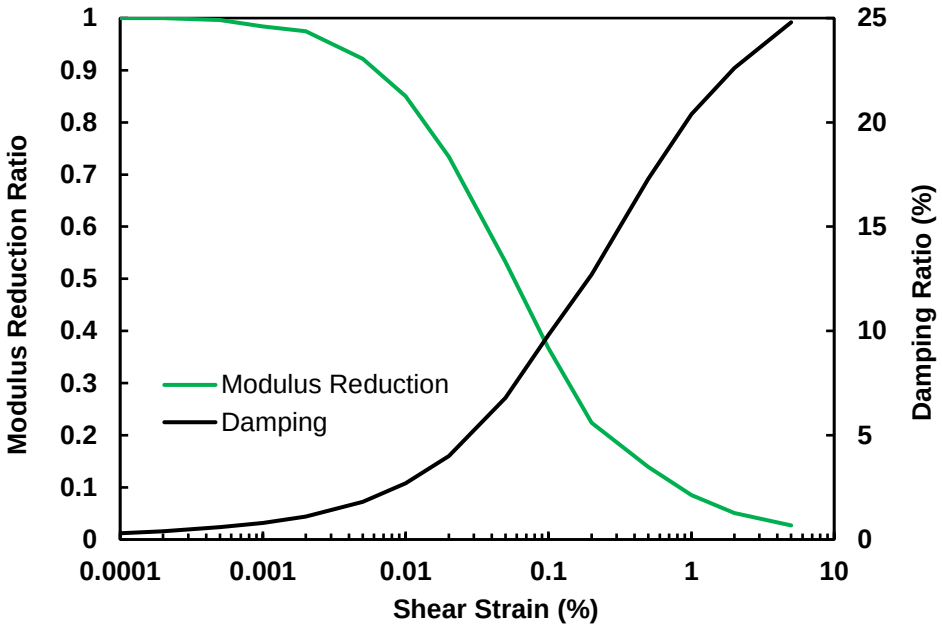

158

159 **Figure 5:** Average modulus reduction ratio and damping ratio adopted for sand (Seed & Idriss, 1970).

160 **3.2 Selection of input motion**

161 Definition of the input motion that is considered for site response analysis of an area requires both subsurface
162 characterization and careful selection of acceleration time histories. In Bhutan, records of acceleration time
163 histories are very rare, if not absent. In the absence of a national seismic code, Bhutan is assumed to fall under
164 Indian seismic zone IV and V, with an expected maximum PGA of 0.24 g and 0.36 g for design purposes. For
165 the two zones mentioned, the PGA for earthquakes with a return period of 475 years is expected to be half of the
166 maximum considered earthquake (MCE), i.e., 0.12 g and 0.18 g. Notably, the GSHAP depicts the PGA range
167 between 0.2-0.28g with an increasing trend in the east of the country. Considering the variations in expected
168 PGA, we selected six acceleration time histories as input motions with PGA ranging from 0.067 g to 0.422 g,
169 considering the lowest and the highest range of possible earthquake scenarios (Table 3). The acceleration time
170 histories used for the 1D ground response analysis are shown in Fig. 6 in ascending PGA order using the
171 ProShake 2.0 computer program. In the ProShake 2.0 program, input motion and soil profile are denoted as "M"
172 and "P", respectively, and are annotated in the subsequent sections (Table 3). The amplitude and frequency
173 content of the bedrock level motion are particularly the most important parameters (Kirtas et al., 2015; Kramer,
174 1996). To understand the strong ground motion characteristics, we plotted the Fourier amplitude versus period
175 in the frequency domain, representing the Fourier amplitude spectra of the input motions, as shown in Fig. 6.
176 The effect of local soils is indicative at a much higher frequency range in all the investigated sites.

177 **Table 3.** Selected strong motion records for ground response analysis.

Event	Station	Year	M_w	PGA (g)	Notation
Loma Prieta/Santa Cruz Mountains	Yerba Buena Island, CA – US Coast Guard	1989	6.9	0.067	M1
Loma Prieta	Diamond Heights	1989	6.9	0.113	M2
Taft Kern County	Taft	1952	7.5	0.185	M3

Northridge	Topanga Fire Station	1994	6.7	0.329	M4
El Centro	Imperial Valley Irrigation District	1940	6.9	0.344	M5
Petrolia	Cape Mendocino	1992	6.6	0.422	M6

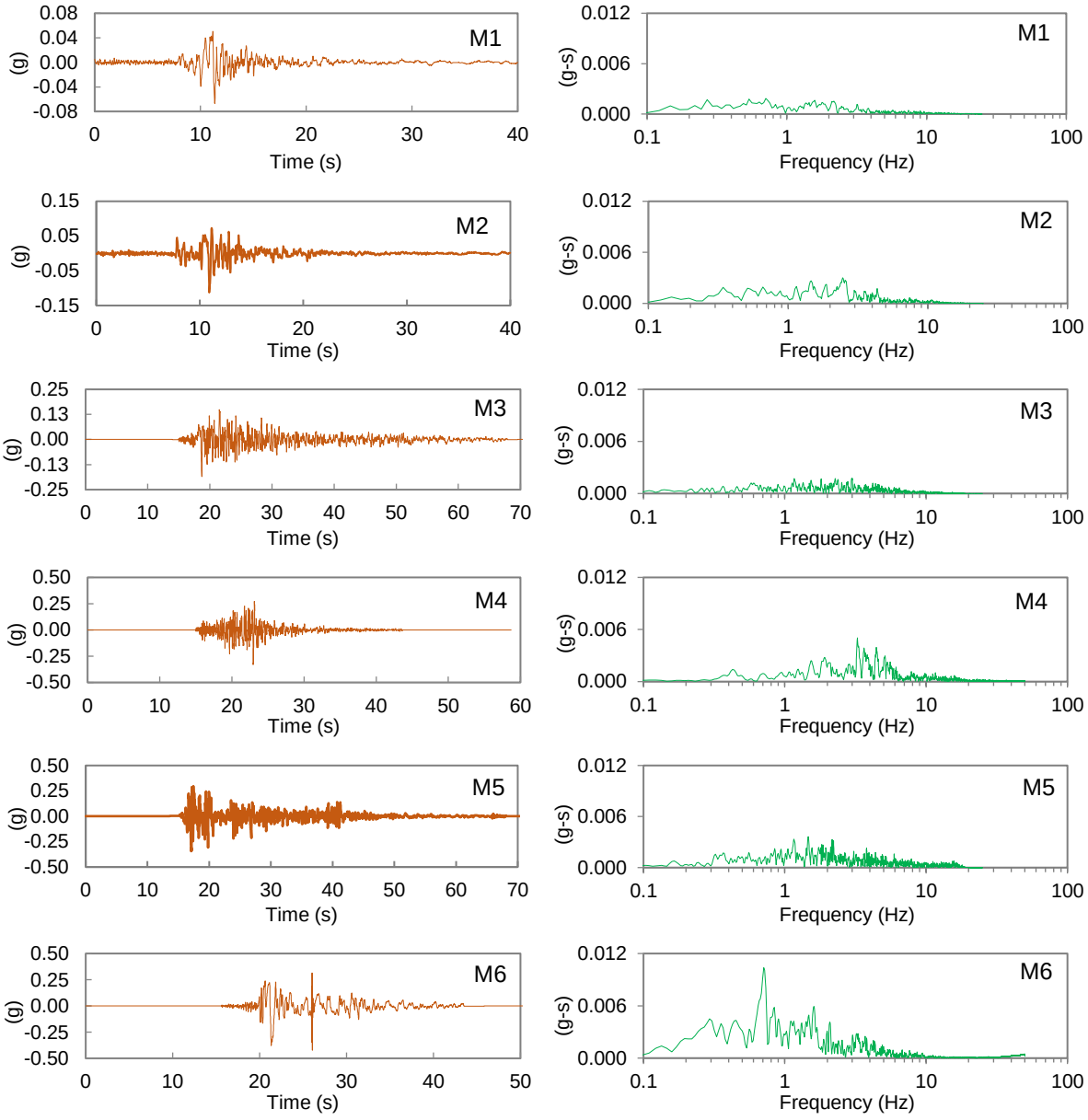

Figure 6: Strong motions and corresponding Fourier amplitude plots of the input ground motions.

3.3 1D ground response analysis

A 1D equivalent linear analysis was performed at eight sites in Phuentsholing, Bhutan to estimate local site effects using the ProShake 2.0 program. In this study, six strong motion records were used to replicate low, medium, and high seismic acceleration categorizes based on the intensity of PGA. The ProShake 2.0 program provides the flexibility to input ground motions and soil profiles and is useful for estimating the outcrop responses to input ground shaking. The improved shear wave velocity profiles down to the engineered bedrock depth (150 m and 400 m) from eight sites were used. The deep shear wave profiles used in this study incorporate

the effects of depth and soil type of visco-elastic soil layers above the predicted engineering bedrock. The 1D ground response analysis accounts for wave propagation from the bedrock outcrop through the visco-elastically stratified soil deposit and provides an estimate of the surface motion parameters. The complex response method is solved by the equation of motion in the frequency domain. Soil nonlinear response is estimated by an iterative quasi-linear procedure in which successive linear analyses are performed while updating the shear modulus and damping ratio based on the shear strain level obtained from the preceding iteration. Iterations continue until the strain-compatible modulus and damping converge.

4. Results and discussion

4.1 Seismic site effects

Figure 7 shows normalized PGAs on surface at two typical locations of the investigated zones. The chart shows depict PGA of 1.2 g to 1.5 g for low PGA earthquakes, 0.7 g to ~1.1 g for medium and high intensity PGA earthquakes. Response parameters can be defined and characterized based on the amplitude parameters of the ground motion and the severity of the ground motion excitation in nearby structures. This in turn is a function of the amplitude or intensity, the frequency content, and the duration of the ground motion (Bradley, 2011). Natural periods or frequency domain parameters are related to the seismic behavior of structures and indirectly reflect the ground motion characteristics (Zafarani et al., 2020). Hence, to commensurate this relationship, the response spectra of bedrock and surface motion are presented in Fig. 8 and 9. The results of various input ground motions indicate a higher spectral acceleration of the soil profile in the period range between 0.3 s to 3.0 s with the peak spectral acceleration of 0.14 g to 1.62 g. Thus, the structures with similar fundamental vibration period are likely to be exposed to greater peak spectral acceleration.

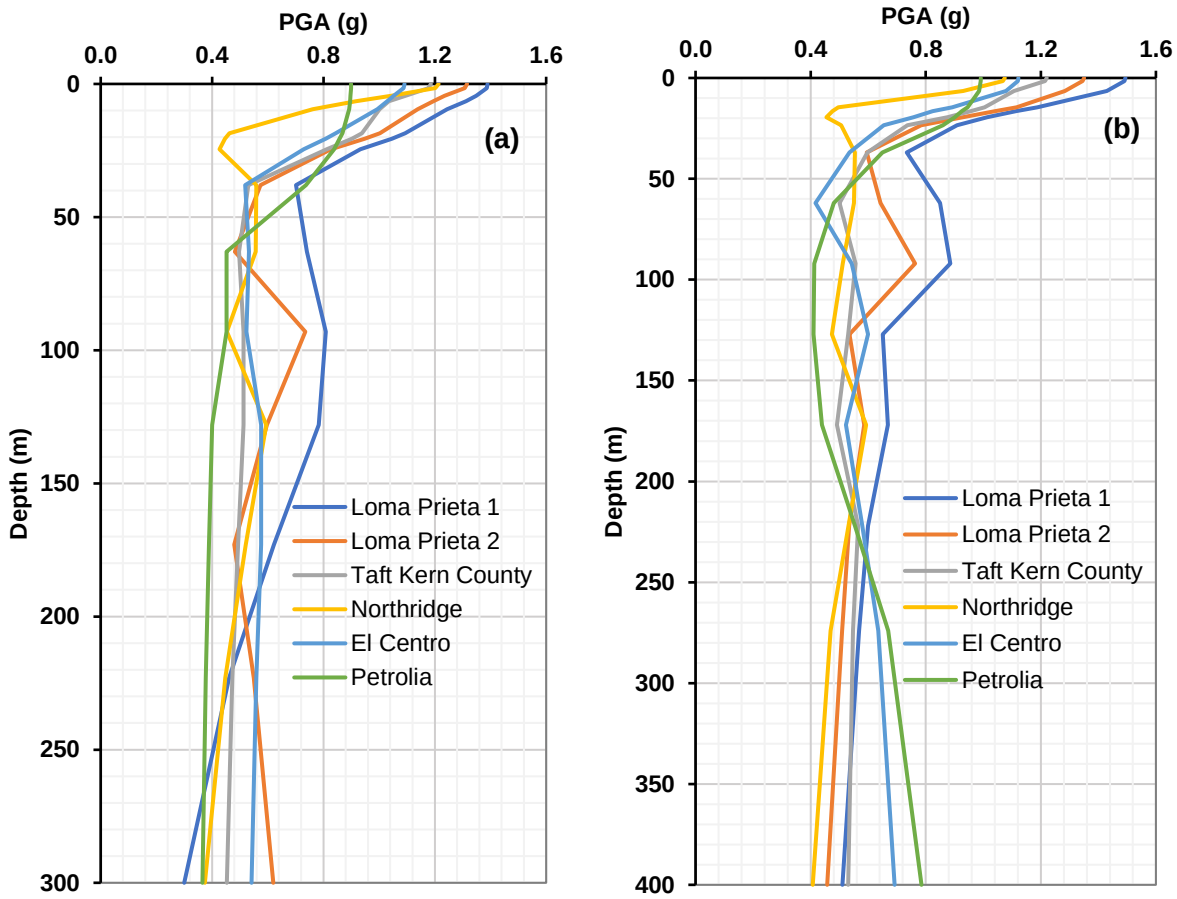

212

213 **Figure 7:** The typical profiles of normalized peak ground acceleration (PGA), (a) Toorsa II in Zone I, and (b)
214 CST Football Ground in Zone II.

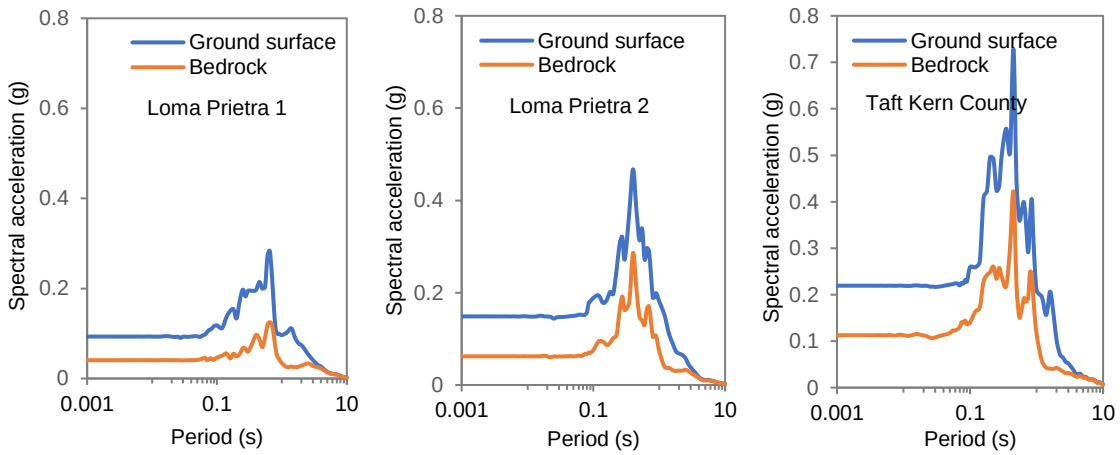

215

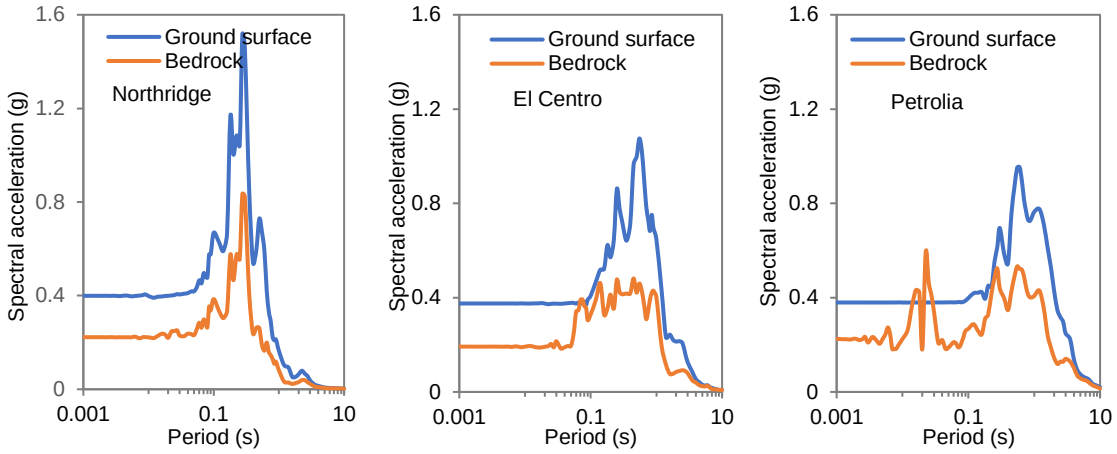

Figure 8: Typical spectral acceleration of bedrock and ground surface motion at Toorsa II in Zone I corresponding to the respective input motions.

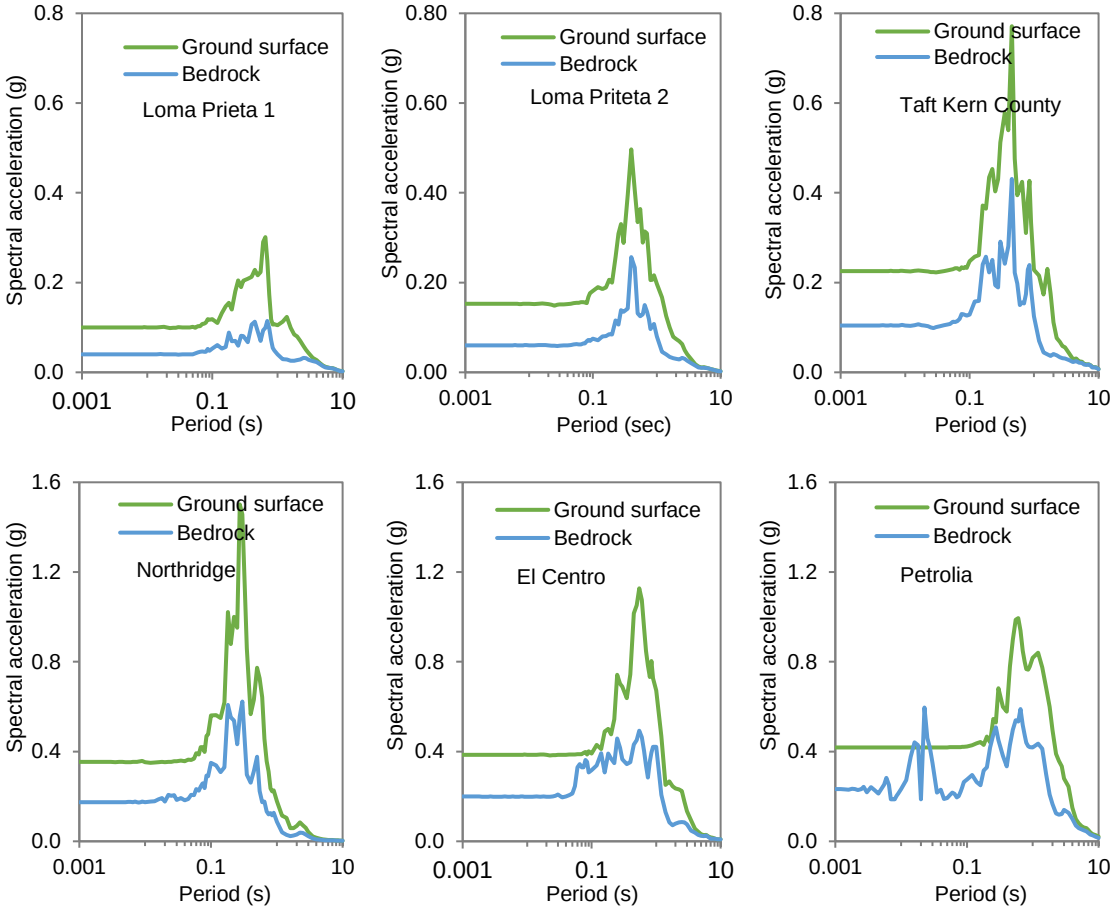

Figure 9: Typical spectral acceleration of bedrock and ground surface motion at CST Football Ground in Zone II corresponding to the respective input motions.

Figures 10 and 11 show the results of typical amplification factors at two locations in the study area. The amplification factors range from 0.7 to 2.7, 0.6 to 2.6, 0.75 to 2.5, and 0.7 to 3.2 for Toorsa II, Dhamdhara I, CST football ground, and Phajoding respectively for 0.01 s to 0.1 s natural period. In the natural period range

from 0.1 to 1.0 s, the amplification factors are in the range from 1.1 to 3.6, 0.7 to 4.2, 1.0 to 3.7, and 1.2 to 5.2 for Toorsa II, Dhamdhara I, CST football ground, and Phajoding, respectively. In the high natural period range, the amplification factors are 5.0, 6.2, and 5.8 for Toorsa II, Dhamdhara I, and CST football ground, respectively. However, in the Phajoding the amplification factor is ~ 1.7 due to a much stiffer soil deposit ($V_{s,30}$ = 584.76 m/s) and shallow engineering bedrock at 150 m.

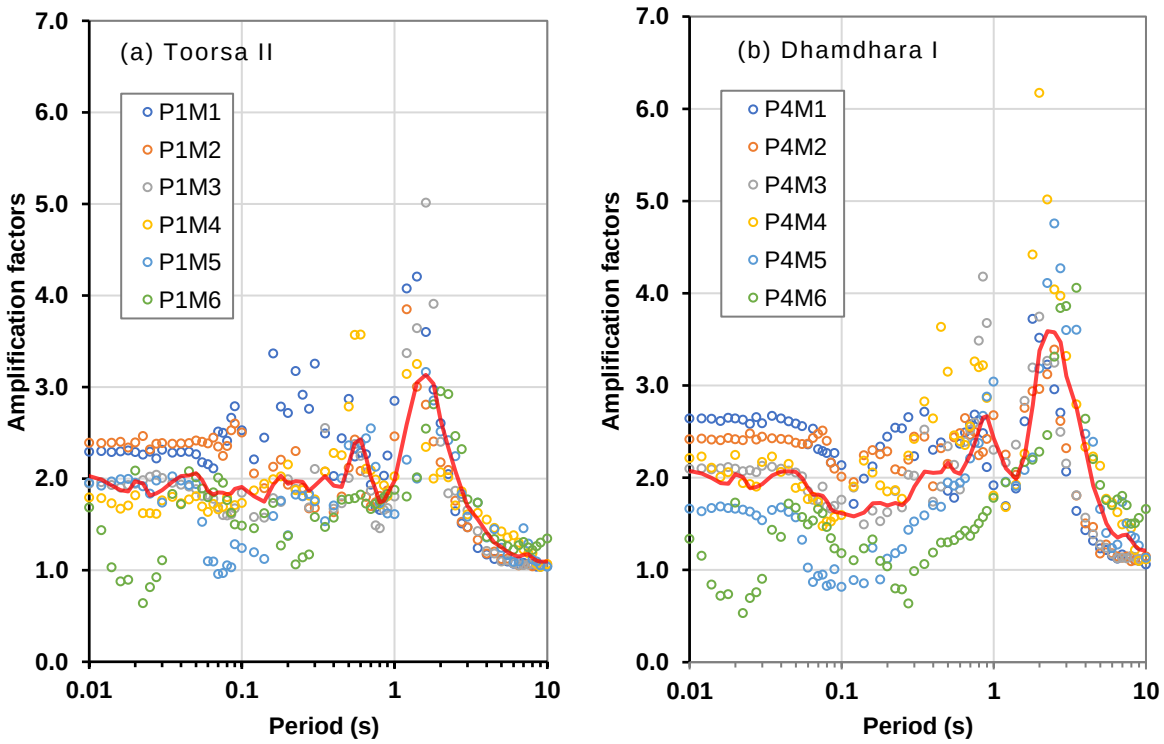

Figure 10: Examples of amplification factors for various earthquakes at (a) Soil profile P1 at Toorsa II in Zone I, (b) Soil profile P4 at Dhamdhara I in Zone I

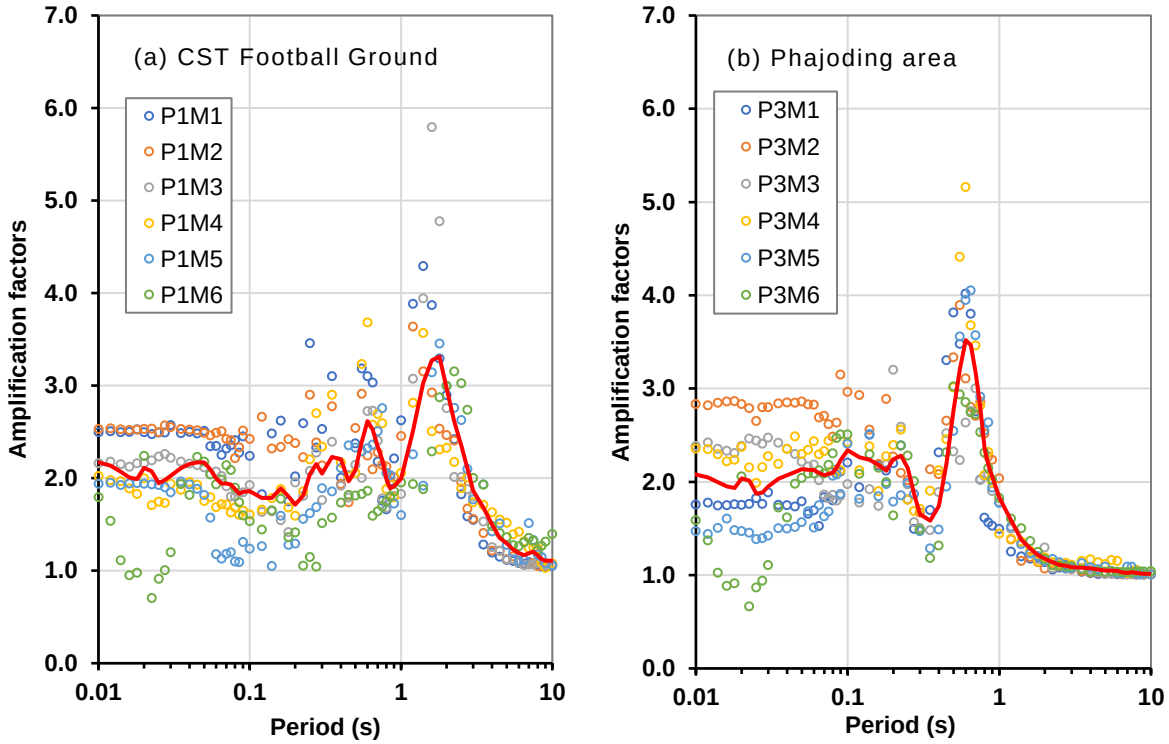

Figure 11: Examples of amplification factors for various earthquakes at (a) Soil profile P1 at CST Football Ground in Zone II, (b) Soil profile P3 at Phajoding in Zone II

4.2 Correlation analysis

The main objective of this study is to demonstrate the sensitivity of input motion amplitudes to predict the variability of seismic site effects due to local ground conditions. We aim to examine potential trends, patterns, and relationships between data sets for the results obtained from the analysis. Using statistical analysis, variation of amplitude parameters is projected by box plots (Figs. 12 and 13). Statistical correlations are fitted between peak ground acceleration (PGA), peak ground velocity (PGV), peak ground displacement (PGD), and spectral acceleration (S_a) to determine the correlation between the effects of strong ground motion and the local soil conditions. As anticipated, the 1992 Petrolia earthquake with 0.422 g PGA (Mw = 6.6) led to the greatest response. However, the 1994 Northridge earthquake with a PGA of 0.329 g (Mw = 6.7) shows greater variability in spectral acceleration compared to other earthquakes. This is because the spectral acceleration is one of the most important response parameters corresponding to the interaction between the ground and the shaking intensity of an earthquake and is directly related to the response of equivalent SDOF systems. Therefore, from the perspectives of seismic site effects the box plot of the spectral acceleration (period or frequency domain) is highly scattered with the outliers, confirming uncertainty in the ground response characteristics in both regions. The El Centro and Petrolia earthquakes, with the highest PGAs, also appear to be closely associated with spectral acceleration.

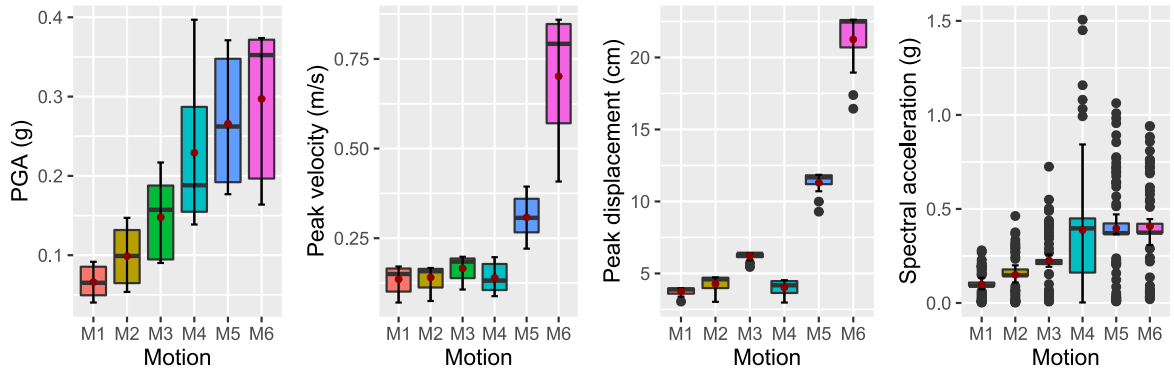

Figure 12: Box and Whisker plot for ground motion parameters of soil profile at P1 Toorsa II in Zone I.

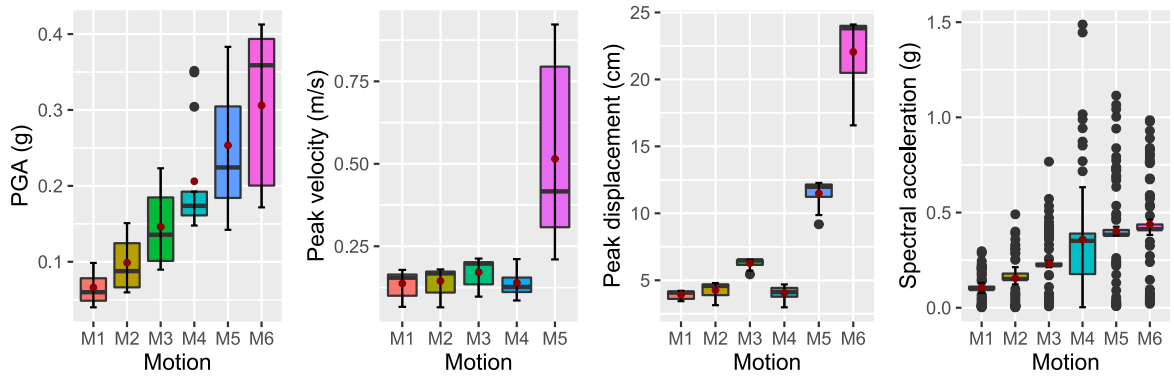

Figure 13: Box and Whisker plot for ground motion parameters of the soil profile at P1 CST Football Ground in Zone II.

Primarily, propagating energy waves (outcrop motion) act on each stratified soil layers that amplifies or de-amplifies the ground motion response parameters at each layer. The sensitivity of the input motions is critically monitored, and enhanced correlation are developed. To outline this, a linear regression model for bedrock outcrop motion and the predicted motion parameters as a function of bedding depth is developed. Regression analysis is performed for one particular soil profile from two zones (Toorsa II and CST Hostel) in order to accurately substantiate sensitivity analysis (Figs. 14 and 15).

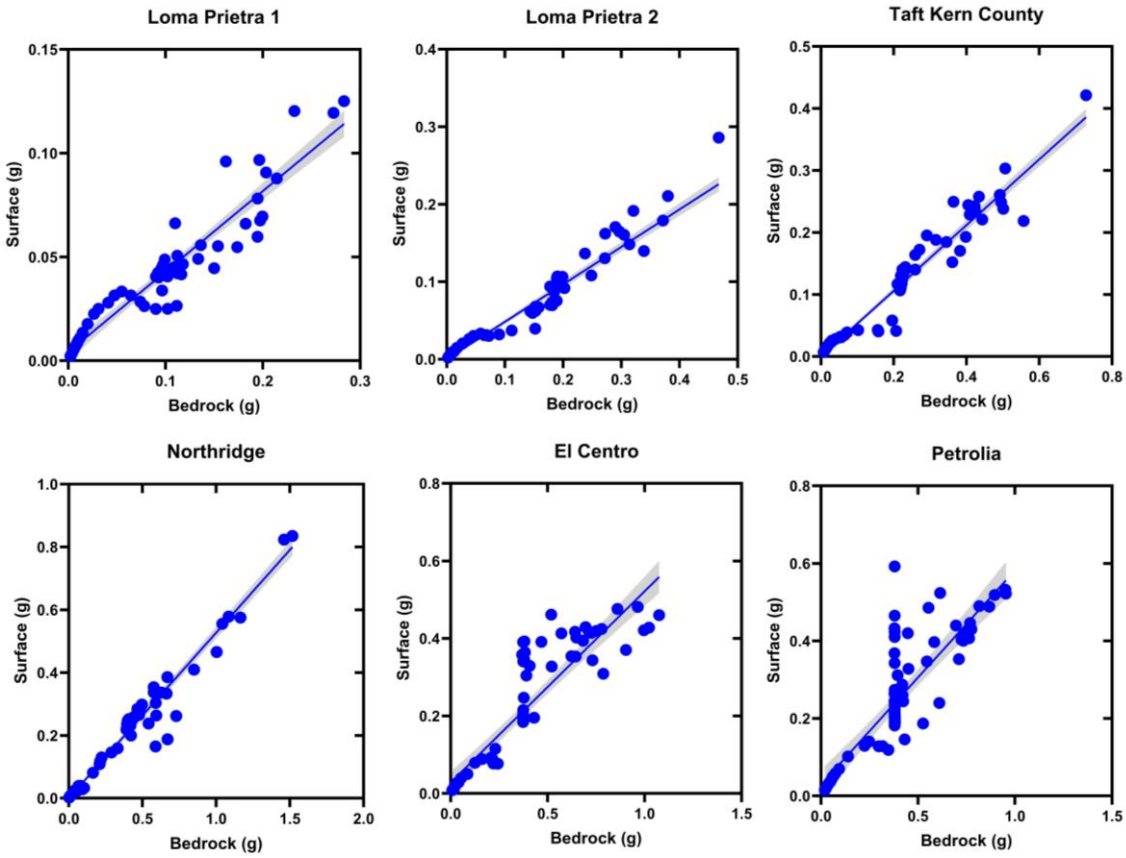

Figure 14: Linear regression model for bedrock and surface spectral accelerations for Toorsa II (Zone I)

The 95% confidence interval (CI) shows a linear relationship for the Loma Prieta 2, Taft Kern County, and Northridge earthquakes indicate a closer impact on surface motion that corresponds to outcrop motion. In this case, the predominant frequency content of the input motion is between 1 and 10 Hz. In contrast, the Loma Prieta 1, El Centro, and Petrolia earthquakes, with a predominant frequency between 0.3 and 1.2 Hz, exhibit typical nonlinearity throughout the spectral range, indicating possible damping of the spectral responses of the soil deposits.

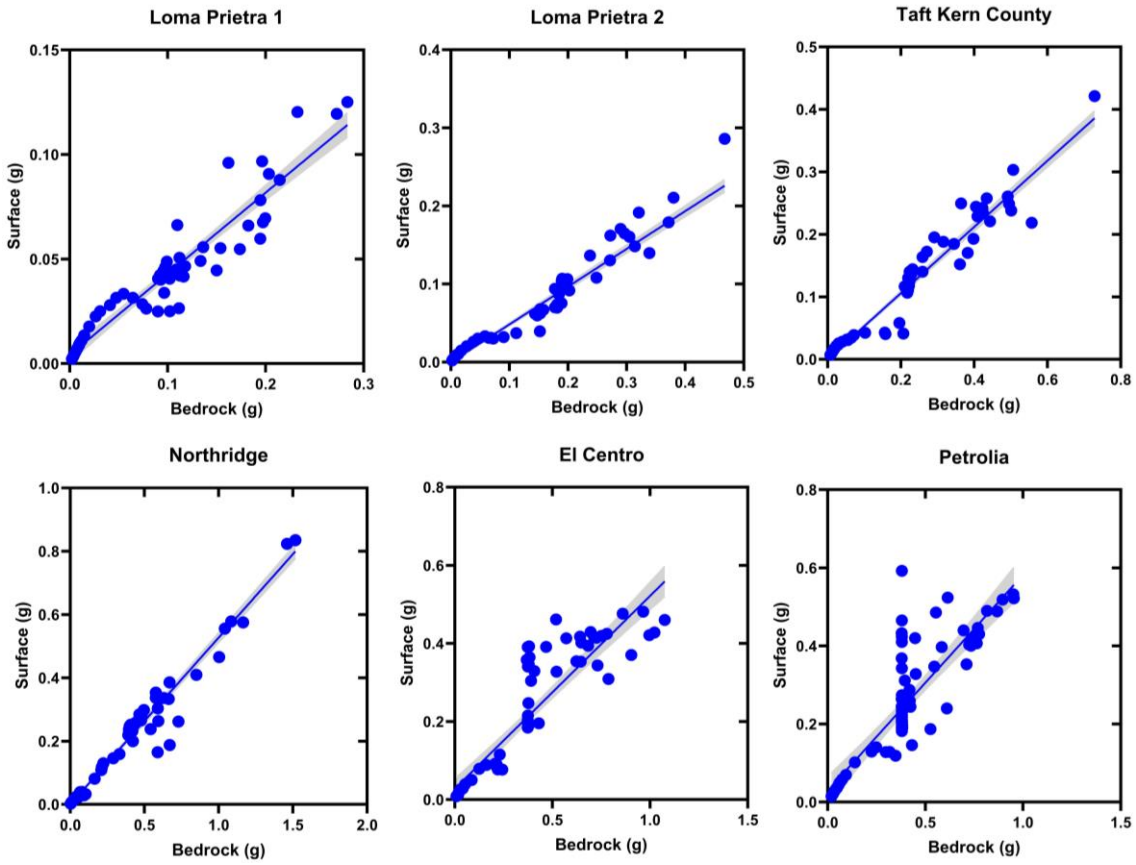

Figure 15: Linear regression model for bedrock and surface spectral accelerations for CST Hostel (Zone II)

Sensitivity of input motion.

Since all analysis sites are in type B site, the trend of ground motion variation to surface is very similar, so the average values may be crucial for better implementation of the scenario-based seismic risk in the study area. Ground response parameters such as PGA and response spectrum intensity including Arias intensity show linear variation for aggregated values while increasing intensity of earthquake shaking corresponding to a given soil profile. The mean, median and standard deviation of the output parameters are computed. The response spectrum intensity is computed based on Housner approach (Housner, 1959) as integral from 0.1 to 2.5 s of the pseudo-velocity spectrum that provides an indication of the average velocity for most civil engineering structures. The plot of sensitivity of various input motions on amplitude parameters to different local soils in two study zones is shown in Figs. 16 and 17.

The standard deviation is lower for a set of predominant natural periods for a soil profile compared to the response spectrum dataset and this deviation from the mean value indicates a stronger soil response to the SDOF systems, as shown in Table 4 and Table 5. Soil nonlinearity often shows a significant scatter in spectral acceleration at higher and lower periods, and therefore the practical reliability of the result is that it prompts more analysis with many input motions to predict the mean (or median) response with some level of confidence (Kramer et al., 2012). The sensitivity of input motion is shown in Figs. 14 and 15 from two investigated locations. The results of the correlation analysis and the sensitivity plots indicate that the input motion M4 (Northridge) has a significant influence on most of the response parameters. The additional ground response parameters are provided in the appendix (Tables A1 and A2).

293 **Table 4.** Descriptive statistics for averaged ground response parameters in Zone I for all four soil profiles and
294 six input ground motions.

	PGA (g)	Aries intensity (m/sec)	Response spectrum intensity (g^2)	Predominant period (sec)	Mean frequency (Hz)
Mean	0.270	1.073	2.996	0.818	3.527
Median	0.238	0.630	2.450	0.689	3.319
Standard deviation	0.121	0.765	2.013	0.468	1.097
84^{th} percentile	0.407	2.215	4.541	1.251	4.824
16^{th} percentile	0.139	0.179	1.322	0.379	2.283

295

Table 5. Descriptive statistics for averaged ground motion parameters in Zone II for all four soil profiles and six input ground motions.	PGA (g)	Arias intensity (m/s)	Response spectrum intensity (g^2)	Predominant period (s)	Mean frequency (Hz)
Mean	0.271	1.079	2.985	0.812	3.814
Median	0.237	0.622	2.417	0.684	3.538
Standard deviation	0.126	0.794	2.066	0.453	1.382
84^{th} percentile	0.411	2.226	4.541	1.243	5.330
16^{th} percentile	0.136	0.174	1.287	0.377	2.349

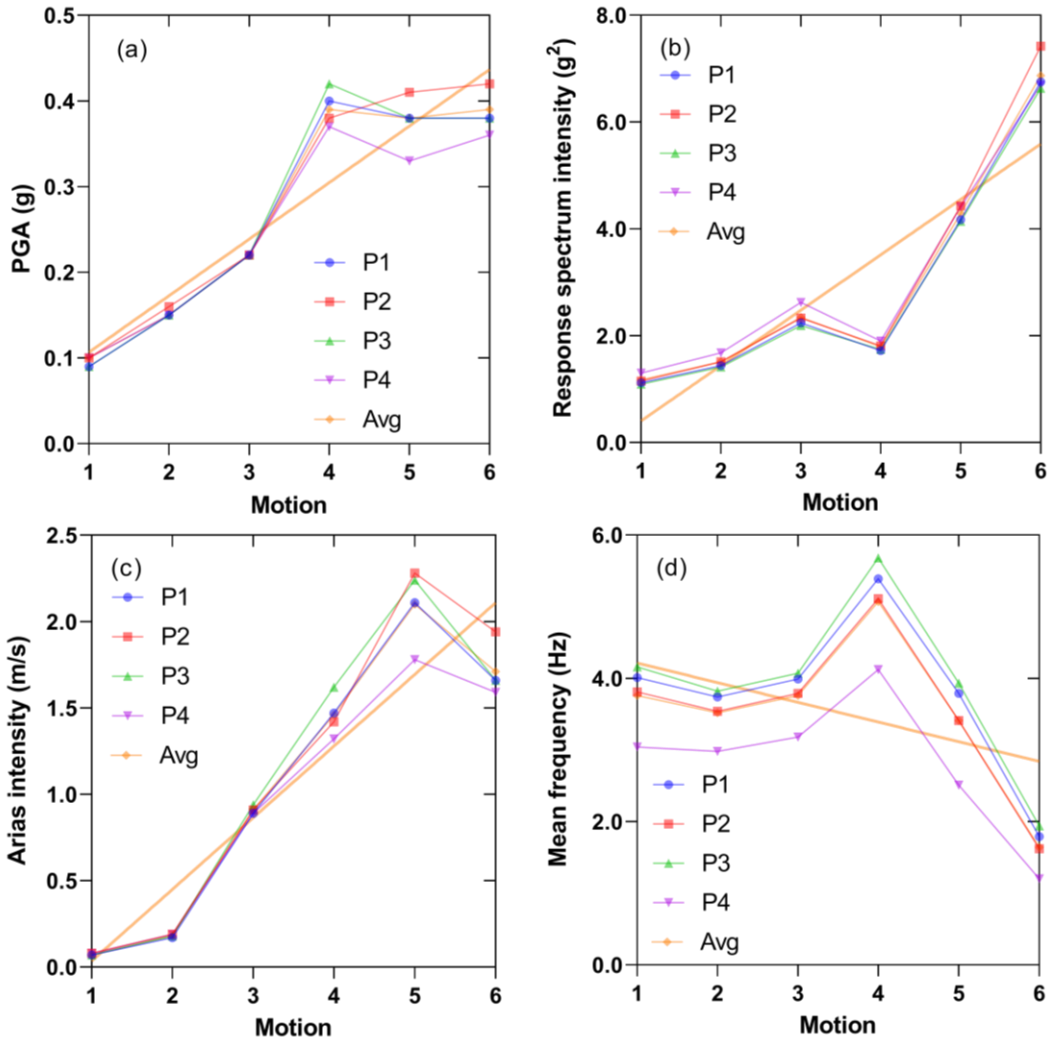

296

297 **Figure 16:** Sensitivity of input ground motion in Zone I. (a) Peak ground acceleration, (b) Response spectrum
298 intensity, (c) Arias intensity, (d) Mean frequency. Soil profiles P1: Toorsa II, P2: Toorsa 1, P3: Dhamdhara II
299 and P4: Dhamdhara I.

300

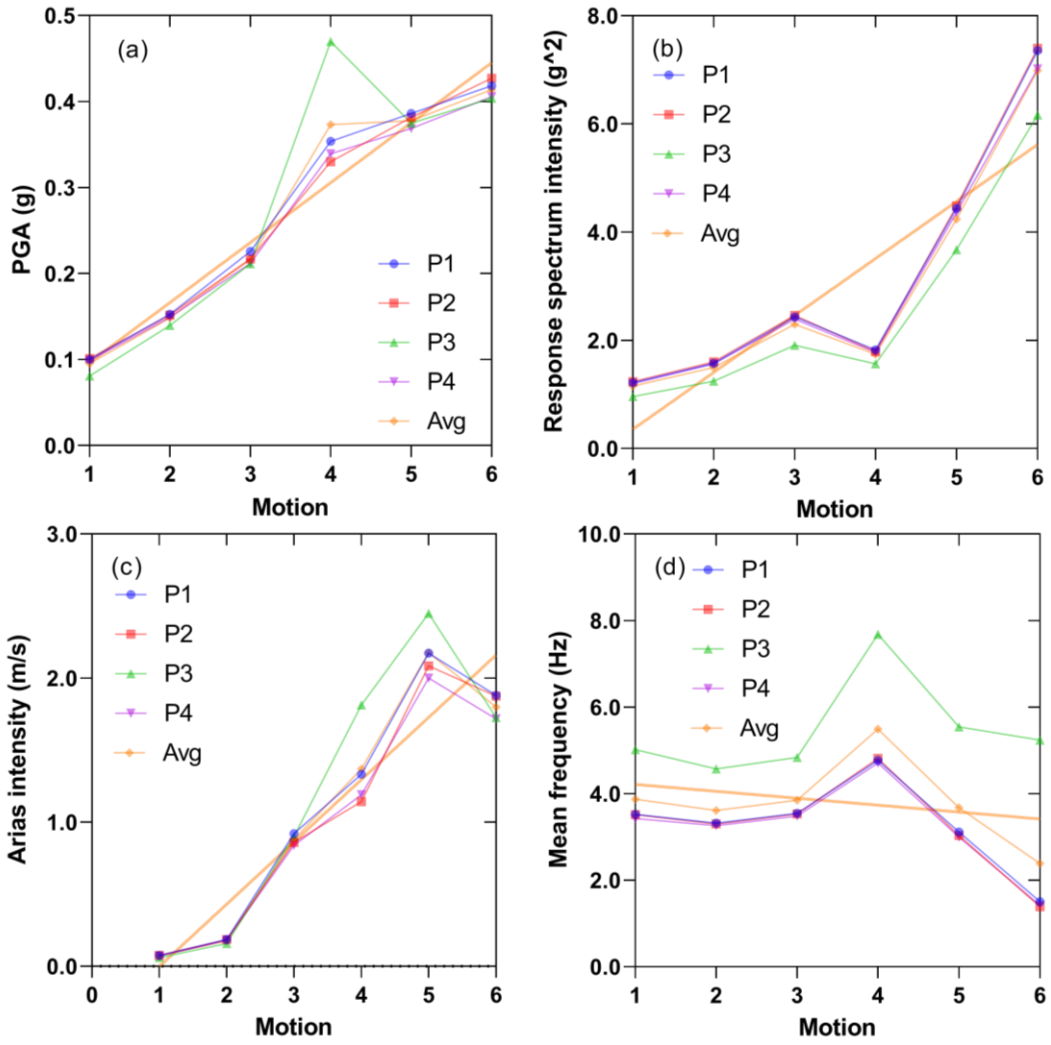

Figure 17: Sensitivity of input ground motion in Zone II. (a) Peak ground acceleration, (b) Response spectrum intensity, (c) Arias intensity, (d) Mean frequency. Soil profiles P1: CST Football Ground, P2: CST Hostel, P3: Phajoding, and P4: Monastery area

In this study, the PGA of M4 Northridge are mapped to show the spatial variability in two zones as shown in Fig. 18. The PGA in Zone I are distributed between 0.37 g to 0.42 g. The variability of PGA in Zone II is higher compared to Zone I, resulting in the range 0.33 g to 0.47 g. The resulting interplay of strong ground motion with local soil conditions primarily highlights the importance of the current study on the significance of input motion characterization.

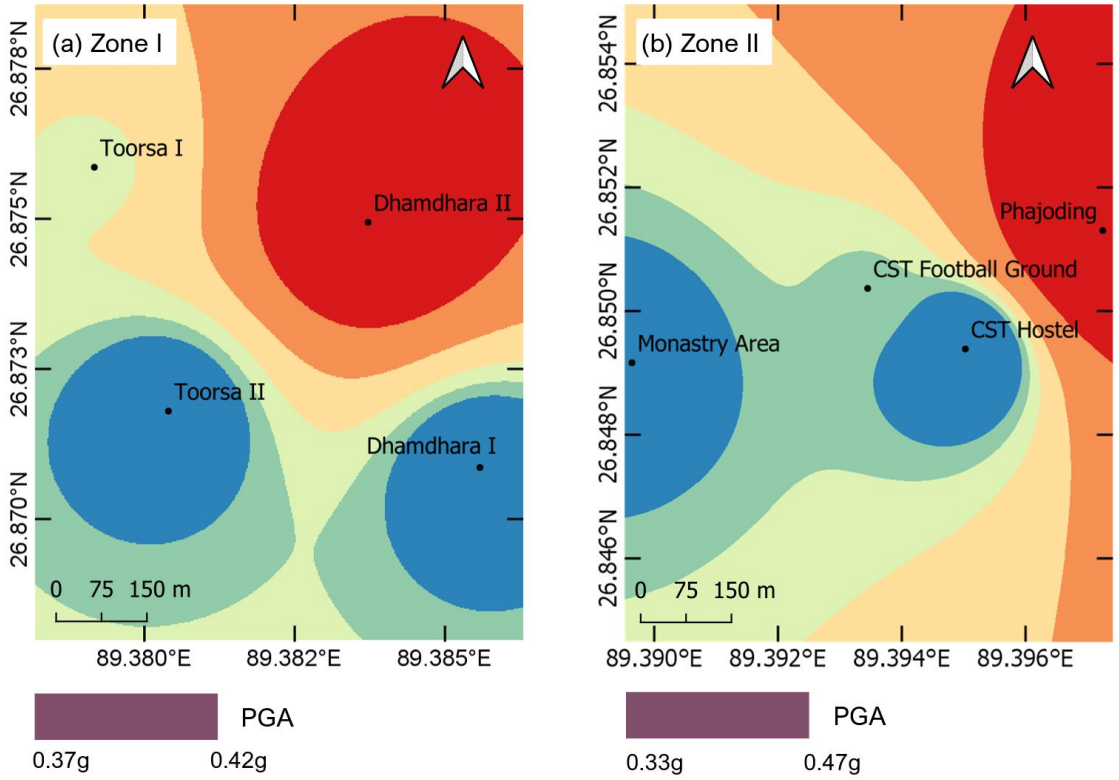

Figure 18: PGA distribution map of input motion M4 Northridge earthquake, (a) Toorsa and Dhamdhara in Zone I, (b) Rinchending in Zone II.

5. Conclusions

Using 1D site response analysis, we perform sensitivity of various input motions. The study concludes the following:

- The trend in the variation of ground motion parameters such as PGA, PGD, PGV and SA projects an increasing order with ground motion intensity as expected. The correlation analysis and linear regression models provide the enhanced characteristics of input motion propagation, indicating possible use of earthquake PGA between 0.11 g and 0.33 g from 1 to 10 Hz frequency.
- The surface PGA in the investigation area of site classification type B shows 0.1 g to 0.15 g for the earthquake of low intensity, 0.23 g to ~ 0.38 g for the earthquake of medium intensity, and more than 0.43 g for an earthquake of high PGA earthquakes. The result shows a higher spectral acceleration in a period range from 0.3 s to 3.0 sec with approximately 0.14 g to 1.62 g peak spectral acceleration.
- The critical range of the fundamental natural period is roughly between 0.9 sec to ~ 5.0 sec with the highest range of seismic wave amplification being between ~ 2.8 to 6.2. In Phajoding, the significance of amplification is comparatively less at ~ 1.7 between 0.4 s and 1.0 s due to a much stiffer soil deposit ($V_{s,30}$ = 584.76 m/s) and a shallow engineering bedrock at 150 m.
- This study indicated some anomalies in seismic site effects due to input motion. Therefore, an appropriate ground motion characterization is recommended for site-specific seismic analysis. The high Fourier amplitude characteristics at low frequency have a greater tendency to reflect anomalies in response parameters.

Data availability

All the data used in this study are presented in the paper.

Author contribution

Conceptualization (KT), Data curation (KT), Formal analysis (KT), Funding acquisition (KRA), Methodology (KT, DG and GF), Resources (KT, DG and KRA), Software and visualization (KT), Writing – original draft preparation (KT), Writing – review & editing (DG, NC, GF and KRA).

Competing interests

The authors declare that they have no competing interests.

Acknowledgements

The authors are thankful to Phuentsholing Thromde (Municipal office) for providing additional geotechnical data.

References

Berthet, T., Hetényi, G., Cattin, R., Sapkota, S. N., Champollion, C., Kandel, T., Doerflinger, E., Drukpa, D., Lechmann, S., and Bonnin, M.: Lateral uniformity of India Plate strength over central and eastern Nepal, Geophysical Journal International, 195(3), 1481–1493, https://doi.org/10.1093/gji/ggt357, 2013.

Bhutani, M., and Naval, S.: Preliminary amplification studies of some sites using different earthquake motions, Civil Engineering Journal (Iran), 6(10), 1906–1921, https://doi.org/10.28991/cej-2020-03091591, 2020.

Bommer, J. J., and Martinez-Pereira, A.: Strong-motion parameters: definition, usefulness and predictability, 12th World Conference on Earthquake Engineering, 1–8, http://www.iitk.ac.in/nicee/wcee/article/0206.pdf, 2000.

Bradley, B. A.: Empirical correlation of PGA, spectral acceleration and spectrum intensities from active shallow crustal earthquakes, Earthquake Engineering and Structural Dynamics, 40(15), 1–15. https://doi.org/10.1002/eqe, 2011.

Chavez-Garcia, F. J., Pedotti, G., Hatzfeld, D., and Bard, P. Y.: An experimental study of site effects near Thessaloniki (northern Greece), Bulletin - Seismological Society of America, 80(4), 784–806, 1990.

Chettri, N., Gautam, D., and Rupakhety, R.: From Tship Chim to Pa Chim: Seismic vulnerability and strengthening of Bhutanese vernacular buildings, In R. Rupakhety and D.Gautam (Ed.), Masonry Construction in Active Seismic Regions (1st ed. Ca, Issue May, pp. 253–288), Elsevier, https://doi.org/10.1016/c2019-0-02453-3, 2021. a

Chettri, N., Gautam, D., and Rupakhety, R.: Seismic vulnerability of vernacular residential buildings in Bhutan, Journal of Earthquake Engineering, 26(1), 1–16. https://doi.org/10.1080/13632469.2020.1868362, 2021. b

Darendeli, M. B.: Development of a New Family of Normalized Modulus Reduction and Material Damping Curves, Dept. of Civil Eng., Univ. of Texas, Austin, 2001

Dobry, R., and Vucetic, M.: Dynamic properties and seismic response of soft clay deposits, International Symposium on Geotech., Eng. of Soft Soils, Maxico, 2(January 1987), 51–87, 1982.

Douglas, J.: Selection of strong-motion records for use as input to the structural models of VEDA, BRGM, 2006.

Drukpa, D., Velasco, A. A., and Doser, D. I.: Seismicity in the Kingdom of Bhutan (1937-2003): Evidence for crustal transcurrent deformation, Journal of Geophysical Research: Solid Earth, 111(6), 1–14, https://doi.org/10.1029/2004JB003087, 2006.

EduPro Civil Systems Inc.: ProShake: Ground Response Analysis Program 2.0, User's Manual. 2017.

Gautam, D.: Mapping surface motion parameters and liquefaction susceptibility in Tribhuvan International Airport, Nepal, Geomatics, Natural Hazards and Risk, 8(2), 1173–1184, https://doi.org/10.1080/19475705.2017.1305993, 2017.

Gautam, D., and Chamlagain, D.: Preliminary assessment of seismic site effects in the fluvio-lacustrine sediments of Kathmandu valley, Nepal, Natural Hazards, 81(3), 1745–1769, https://doi.org/10.1007/s11069-016-2154-y, 2016.

Gautam, D., Forte, G., and Rodrigues, H.: Site effects and associated structural damage analysis in Kathmandu Valley, Nepal. Earthquake and Structures, 10(5), 1013–1032, https://doi.org/10.12989/eas.2016.10.5.1013, 2016.

Housner, G.W.: Behavior of structures during earthquakes, Journal of the Engineering Mechanics Division, ASCE, 85(14), 109-129, 1959.

ISSMGE.: Manual for zonation on seismic geotechnical hazards. In: Technical committee for earthquake geotechnical engineering, TC4, international society for soil mechanics and geotechnical engineering, The Japanese Geotechnical Society, Tokyo,1999.

IS:1893.: Criteria for Earthquake Resistant Design of Structures - General Provisions and Buildings Part-1, Bureau of Indian Standards, New Delhi, Part 1, 1–39, 2002.

Jishnu, R. B., Naik, S. P., Patra, N. R., and Malik, J. N.: Ground response analysis of Kanpur soil along Indo-Gangetic Plains, Soil Dynamics and Earthquake Engineering, 51(2013), 47–57, https://doi.org/10.1016/j.soildyn.2013.04.001, 2013.

Kirtas, E., Koliopoulos, P., Kappos, A., Theodoulidis, N., Savvaidis, A., Margaris, B., and Rovithis, E.: Identification of earthquake ground motion using site effects analysis in the case of Serres city, Greece, International Journal of Civil Engineering and Architecture, 2(1), 20–27, 2015.

Kramer, S. L.: Geotechnical Earthquake Engineering, Prentice Hall, 1996.

Kramer, S. L., Arduino, P., and Sideras, S. S.: Earthquake ground motion selection, The State of Washington Department of Transportation, 2012.

Long, S., and McQuarrie, N.: Placing limits on channel flow: Insights from the Bhutan Himalaya, Earth and Planetary Science Letters, 290(3–4), 375–390, https://doi.org/10.1016/j.epsl.2009.12.033; 2010.

Lopez-Caballero, F., Gelis, C., Regnier, J., and Bonilla, L. F.: Site response analysis including earthquake input ground motion and soil dynamic properties variability, 15th World Conference on Earthquake Engineering, 2012.

Licata, V., Forte, G., d'Onofrio, A., Santo, A., Silvestri, F.: A multi-level study for the seismic microzonation of the Western area of Naples (Italy), Bulletin of Earthquake Engineering, 17(9), 4711–4741, 2019.

McQuarrie, N., Long, S. P., Tobgay, T., Nesbit, J. N., Gehrels, G., and Ducea, M. N.: Documenting basin scale, geometry and provenance through detrital geochemical data: Lessons from the Neoproterozoic to Ordovician Lesser, Greater, and Tethyan Himalayan strata of Bhutan, Gondwana Research, 23(4), 1491–1510, https://doi.org/10.1016/j.gr.2012.09.002, 2013.

Naik, S. P., and Patra, N. R.: Generation of Liquefaction Potential Map for Kanpur City and Allahabad City of Northern India: An Attempt for Liquefaction Hazard Assessment, Geotechnical and Geological Engineering, 36(1), 293–305, https://doi.org/10.1007/s10706-017-0327-4, 2018.

Nath, S. K., and Thingbaijam, K. K. S.: Seismic hazard assessment - A holistic microzonation approach, Natural Hazards and Earth System Science, 9(4), 1445–1459, https://doi.org/10.5194/nhess-9-1445-2009, 2009.

Panjamani, A., Katukuri, A. K., Reddy, G. R., Moustafa, S. S. R., and Al-Arifi, N. S. N.: Seismic site classification and amplification of shallow bedrock sites, PLoS ONE, 13(12), 1–22, https://doi.org/10.1371/journal.pone.0208226, 2018.

Puri, N., Jain, A., Mohanty, P., and Bhattacharya, S.: Earthquake Response Analysis of Sites in State of Haryana using DEEPSOIL Software, Procedia Computer Science, 125(January), 357–366, https://doi.org/10.1016/j.procs.2017.12.047, 2018.

Seed, H. B., and Idriss, I. M.: Soil Moduli and Damping Factors for Dynamic Response Analyses [Report No. EERC 70-10], Earthquake Engineering Research Centre, University of California, Berkeley, https://ntrl.ntis.gov/NTRL/dashboard/searchResults/titleDetail/PB197869.xhtml, 1970.

Seed, H. B., Wong, R. T., Idriss, I. M., and Tokimatsu, K.: Moduli and Damping Factors for Dynamic Analyses of Cohesionless Soils, Journal of Geotechnical Engineering, 112(11), 1016–1032, 1986.

Shafiee, A., Kamalian, M., Jafari, M. K., and Hamzehloo, H.: Ground motion studies for microzonation in Iran, Natural Hazards, 59(1), 481–505, https://doi.org/10.1007/s11069-011-9772-1, 2011.

Shiuly, A., and Narayan, J. P.: Deterministic seismic microzonation of Kolkata city. Natural Hazards, 60(2), 223–240, https://doi.org/10.1007/s11069-011-0004-5, 2012.

Sil, A., and Haloi, J.: Site-specific ground response analysis of a proposed bridge site over Barak River along Silchar Bypass Road, India, Innovative Infrastructure Solutions, 3(1), https://doi.org/10.1007/s41062-018-0167-y, 2018.

Sitharam, T. G.: Seismic Microzonation: Principles, Practices and Experiments, Electronic Journal of Geotechnical Engineering, 1–58, 2008.

Sitharam, T. G., Anbazhagan, P., Mahesh, G. U., Bharathi, K., and Reddy, P. N.: Seismic Hazard Studies Using Geotechnical Borehole Data and GIS, Symposium on Seismic Hazard Analysis and Microzonation, 341–358, 2005.

Stevens, V. L., De Risi, R., Le Roux-Mallouf, R., Drukpa, D., and Hetényi, G.: Seismic hazard and risk in Bhutan, Natural Hazards, 104(3), 2339–2367, https://doi.org/10.1007/s11069-020-04275-3, 2020.

Tempa, K., and Chettri, N.: Comprehension of Conventional Methods for Ultimate Bearing Capacity of Shallow Foundation by PLT and SPT in Southern Bhutan, Civil Engineering and Architecture, 9, 375–385, https://doi.org/10.13189/cea.2021.090210, 2021.

Tempa, K., Chettri, N., Gurung, L., and Gautam, D.: Shear wave velocity profiling and ground response analysis in Phuentsholing, Bhutan, Innovative Infrastructure Solutions, 6(2), 1–16, https://doi.org/10.1007/s41062-020-00420-w, 2021.

Tempa, K., Chettri, N., Sarkar, R., Saha, S., Gurung, L., Dendup, T., and Nirola, B. S.: Geotechnical parameter assessment of sediment deposit: A case study in Pasakha, Bhutan, Cogent Engineering, 8(1), 1–21, https://doi.org/10.1080/23311916.2020.1869366, 2021.

Tempa, K., Sarkar, R., Dikshit, A., Pradhan, B., Simonelli, A. L., Acharya, S., and Alamri, A. M.: Parametric study of local site response for bedrock ground motion to earthquake in Phuentsholing, Bhutan, Sustainability (Switzerland), 12(13), 1–20, https://doi.org/10.3390/su12135273, 2020.

Vucetic, M., and Dobry, R.: Effect of Soil Plasticity on Cyclic Response. Journal of Geotechnical Engineering, 117(1), 89–107, http://sokocalo.engr.ucdavis.edu/~jeremic/PAPERSlocalREPO/CM1769.pdf, 1991.

Wyss, M., and Rosset, P.: Mapping seismic risk: The current crisis. Natural Hazards, 68(1), 49–52, https://doi.org/10.1007/s11069-012-0256-8, 2013.

Zafarani, H., Ghafoori, S. M. M., Soghrat, M. R., and Shafiee, M.: Spatial correlation of peak ground motions and pseudo-spectral acceleration based on the sarpol-e-zahab mw 7.3, 2017 earthquake data, Annals of Geophysics, 63(4), 1–15, https://doi.org/10.4401/ag-8349, 2020.